

Entropy of deterministic trajectory via trajectories ensemble

Yonggang Peng(彭勇刚), Cuiping Ran(冉翠平), Yujun Zheng(郑雨军)

Citation: Chin. Phys. B, 2024, 33 (**6**): 063401. DOI: 10.1088/1674-1056/ad3348
Journal homepage: http://cpb.iphy.ac.cn; http://iopscience.iop.org/cpb

What follows is a list of articles you may be interested in

Fragmentation dynamics of electron-impact double ionization of helium

Shiwei Liu(刘士炜), Difa Ye(叶地发), and Jie Liu(刘杰)
Chin. Phys. B, 2023, 32 (**6**): 063402. DOI: 10.1088/1674-1056/acbe33

Development of an electronic stopping power model based on deep learning and its application in ion range prediction

Xun Guo(郭寻), Hao Wang(王浩), Changkai Li(李长楷),Shijun Zhao(赵仕俊), Ke Jin(靳柯), and Jianming Xue(薛建明)
Chin. Phys. B, 2022, 31 (**7**): 073402. DOI: 10.1088/1674-1056/ac4e0c

Surface for methane combustion: $O(^3P)+CH_4 \rightarrow OH+CH_3$

Ya Peng(彭亚), Zhong-An Jiang(蒋仲安), Ju-Shi Chen(陈举师)
Chin. Phys. B, 2020, 29 (**7**): 073401. DOI: 10.1088/1674-1056/ab90f5

Exploring the methane combustion reaction: A theoretical contribution

Ya Peng(彭亚), Zhong-An Jiang(蒋仲安), Ju-Shi Chen(陈举师)
Chin. Phys. B, 2018, 27 (**2**): 023401. DOI: 10.1088/1674-1056/27/2/023401

Optical potential approach for positron scattering by metastable 2^3S state of helium

Xi-Gang Wu(吴锡刚), Yong-Jun Cheng(程勇军), Fang Liu(刘芳), Ya-Jun Zhou(周雅君)
Chin. Phys. B, 2017, 26 (**2**): 023401. DOI: 10.1088/1674-1056/26/2/023401

Entropy of deterministic trajectory via trajectories ensemble

Yonggang Peng(彭勇刚)[†], Cuiping Ran(冉翠平), and Yujun Zheng(郑雨军)[‡]

School of Physics, Shandong University, Jinan 250100, *China*

(Received 3 January 2024; revised manuscript received 6 March 2024; accepted manuscript online 13 March 2024)

We present a formulation of the single-trajectory entropy using the trajectories ensemble. The single-trajectory entropy is affected by its surrounding trajectories via the distribution function. The single-trajectory entropies are studied in two typical potentials, i.e., harmonic potential and double-well potential, and in viscous environment by interacting trajectory method. The results of the trajectory methods are in agreement well with the numerical methods (Monte Carlo simulation and difference equation). The single-trajectory entropies increasing (decreasing) could be caused by absorption (emission) heat from (to) the thermal environment. Also, some interesting trajectories, which correspond to the rare evens in the processes, are demonstrated.

Keywords: trajectory entropy, trajectories ensemble

PACS: 34.10.+x, 05.40.–a **DOI:** 10.1088/1674-1056/ad3348

1. Introduction

The entropy has played important roles in the thermodynamic, statistical mechanics, and information theory, since it is first introduced by Clausius in the middle of 19th century. Clausius employed the entropy to describe the transition direction between two equilibrium states in thermodynamics.[1,2] Boltzmann defined the entropy as a function of the number of micro-states of the system.[3–6] Later, Gibbs gave the other definition of the entropy based on the probabilities of the microstates.[7] The relationship between Boltzmann entropy and Gibbs entropy has been discussed by Jaynes[8] and Zupanovic.[9] Shannon employed the entropy to describe the uncertainty of the bits in the information transition,[10] and nowadays, Shannon's entropy becomes the key concept in the information theory. In Ref. [11], von Neumann introduced quantum entropy to describe the quantity of the quantum information contained in a quantum state.

With the development of the experimental techniques, one can track the trajectory of single molecule in matrix or solution.[12–16] The concepts of thermodynamics are employed to study behavior of single molecules. The concept of entropy is extended into the non-equilibrium system,[17] such as fluid dynamical systems, nonlinear dynamical systems, thermal driving dynamical systems, and biological systems.[12,13,15,16,18,19] In single molecule level, such as the colloid particles, biomolecules, polymers, enzymes, and molecular motors, in an aqueous solution,[20] dynamical behavior of a system demonstrates stochastic properties. This means that the applied work, internal energy, and dissipated heart should be considered as random variables.[21]

The probability distribution of entropy is connected to the fluctuation theorems,[22–26] such as Jarzynski relation,[27] Crooks theorem,[28] and Hatano–Sasa,[29] which constrains the probability of negative entropy production. The entropy production for the Markov stochastic processes has been studied by Qian and Qian.[30] Seifert introduced a single-trajectory entropy for the stochastic thermodynamics,[31] and several experiments showing the integral and detailed fluctuation theorem are hold for finite times.[32] Recently, more experiments study the entropy on single molecule level, in physics, chemistry, and biophysics.[12–16]

To understand the fluctuation theorem in single-molecule level, the single-trajectory entropy is introduced to study the stochastic non-equilibrium dynamics.[20,31,33] The single-trajectory entropy extends the entropy concept from ensemble to individual level, and the ensemble average over all the single-trajectory entropy gives the classical entropy, in which the fluctuation of the single-trajectory entropy is covered by the averaging.[20] The fluctuation of the quantity reflects the rare events occurring in the stochastic processes.

Many trajectory methods, such as classical trajectory method,[34] semiclassical trajectory method, quantum trajectory method,[35–37] and interacting trajectory method,[38–42] are developed to investigate the dynamical properties of the systems. The advantages of the trajectory methods is effectively to numerically solve the corresponding partial differential equations, also to numerically simulate large quantum systems.[34–39] The interacting trajectory method has been employed to study different dynamical processes, such as anomalous diffusion process,[40] entanglement dynamics,[41] quantum tunneling processes, and autocorrelation function.[42]

In this paper, we present a formulation of the deterministic trajectory entropy using the trajectory ensemble, and study the deterministic trajectory entropy of a particle moving in two

[†]Corresponding author. E-mail: ygpeng@sdu.edu.cn
[‡]Corresponding author. E-mail: yzheng@sdu.edu.cn

© 2024 Chinese Physical Society and IOP Publishing Ltd

typical potentials and viscous environment. Each trajectory is interacting with other trajectories also exchanging energies with other trajectories and the heat bath. The trajectory can exchange heat with the thermal environment, which causes the entropy changing with the evolution time. Several rare interesting trajectories are found, which reflect the exchanging energies via the collision with other trajectories. The results of the interacting trajectory method and of other numerical methods (such as Monte Carlo simulation, difference equation) are in agreement very well. Our study could help to understand thermal properties in the molecular reaction dynamics.

This paper organized as follows: The theoretical framework of the trajectory method is given in Section 2. We present the results of a particle in the harmonic potential and double-well potential for one-dimensional and two-dimensional conditions. Some necessary discussions are presented in Section 3. Finally, the conclusion is given in Section 4.

2. Theoretical framework

The non-equilibrium Gibbs entropy can be written as[31,43]

$$S(t) = -\int \mathrm{d}\Gamma W(\Gamma,t)\ln W(\Gamma,t), \tag{1}$$

where $W(\Gamma,t)$ is the probability density in phase space at point Γ and time t. Generally, the probability density $W(\Gamma,t)$ can be expressed as a series of δ function[39]

$$W(\Gamma,t) = \frac{1}{N}\sum_{j=1}^{N}\delta(\Gamma-\Gamma_j), \tag{2}$$

where N is the number of trajectories, $\delta(\Gamma-\Gamma_j)$ is Dirac δ function. The generalized Dirac δ function as a quasi-distribution function is widely employed in quantum optics,[44] and Γ_j are the sample points in the phase space.

The non-equilibrium Gibbs entropy can be rewritten as

$$\begin{aligned} S(t) &= -\int \mathrm{d}\Gamma W(\Gamma,t)\ln W(\Gamma,t) \\ &= -\frac{1}{N}\sum_{j=1}^{N}\int \mathrm{d}\Gamma\,\delta(\Gamma-\Gamma_j)\ln W(\Gamma,t) \\ &= -\frac{1}{N}\sum_{j=1}^{N}\ln W(\Gamma_j,t), \end{aligned} \tag{3}$$

where $W(\Gamma_j,t)$ is the probability density of the jth trajectory at time t. The deterministic trajectory entropy can be defined as

$$\begin{aligned} s_j(t) &\equiv -\ln W(\Gamma_j,t) \\ &= -\ln\Big(\frac{1}{N}\sum_{k=1}^{N}\delta(\Gamma_j-\Gamma_k)\Big), \end{aligned} \tag{4}$$

Γ_i should satisfy a Hamilton-like equation, which could be considered as a deterministic trajectory in phase space. A stochastic trajectory entropy is defined based on samples of the stochastic processes in coordinate space in Ref. [31]. Then the Gibbs entropy $S(t)$ is the average of the single-trajectory entropies $s_j(t)$,

$$S(t) = \frac{1}{N}\sum_{j=1}^{N}s_j(t). \tag{5}$$

The δ function in the probability density $W(\Gamma_j,t)$ is replaced by a kernel function, such as Gaussian function, Biweight function, Epanechnikov function, in the kernel density estimation theory,[38,39,45,46] namely,

$$W(\Gamma_j,t) = \frac{1}{N}\sum_{k=1}^{N}\kappa(\Gamma_j-\Gamma_k), \tag{6}$$

where $\kappa(x)$ is the kernel function. The single-trajectory entropy can be rewritten as

$$s_j(t) = -\ln W(\Gamma_j,t). \tag{7}$$

Here, we employ the Gaussian kernel function

$$\kappa(x) = \frac{1}{(2\pi)^{\ell/2}h\Delta}\exp\Big(-\frac{x^2}{2h^2\Delta^2}\Big), \tag{8}$$

where $h>0$ is the bandwidth depending on the dimensionality of the data and the kernel functions, such as ℓ-dimensional data and Gaussian kernels, $h=(4/(N(\ell+2)))^{1/(\ell+4)}$.[45,46] Δ is a characteristic length scale of the density function.

For stochastic processes, the probability density can be obtained by the Fokker–Planck equation in phase space,[47–50]

$$\frac{\partial}{\partial t}W = -\frac{p}{m}\frac{\partial}{\partial q}W + V'\frac{\partial}{\partial p}W + \gamma_0\frac{\partial}{\partial p}\Big(p + mk_{\mathrm{B}}T\frac{\partial}{\partial p}\Big)W, \tag{9}$$

where $V'\equiv\partial V/\partial q$ is the derivative of the potential V with respect to q, corresponding to the force exerting on the particle by potential V, m is the mass of the particle, γ_0 is the friction constant, k_{B} is Boltzmann's constant, and T is the absolute temperature of the heat bath.

In the phase space $\{q,p\}$, the probability of a particle appears at (q,p) to $(q+\mathrm{d}q,p+\mathrm{d}p)$ at time t is $W(q,p,t)\mathrm{d}q\mathrm{d}p$, where $W(q,p,t)$ is the probability density at time t. The particle conservation corresponding to the probability density $W(q,p,t)$ in the phase space satisfies the well-known continuity equation

$$\frac{\partial}{\partial t}W(q,p,t) + \nabla\cdot\boldsymbol{j}(q,p,t) = 0, \tag{10}$$

where the divergence operator $\nabla\equiv(\partial/\partial q,\partial/\partial p)$, and $\boldsymbol{j}(q,p,t)$ is the probability flux in phase space, which can be written as

$$\boldsymbol{j}(q,p,t) \equiv \boldsymbol{v}W(q,p,t) = (\dot{q},\dot{p})^{\mathrm{T}}W(q,p,t), \tag{11}$$

where superscript T represents the transpose.

In comparison of Eqs. (10) and (9), one can obtain the divergence of the probability flux as follows:

$$\nabla\cdot\boldsymbol{j}=-\frac{p}{m}\frac{\partial}{\partial q}W+V'\frac{\partial}{\partial p}W+\gamma_0\frac{\partial}{\partial p}\Big(p+mk_{\mathrm{B}}T\frac{\partial}{\partial p}\Big)W. \quad (12)$$

Combining with Eq. (11), one could finally obtain

$$\dot{q}=\frac{p}{m},\ \ \dot{p}=-V'-\gamma_0 p-\gamma_0 mk_{\mathrm{B}}T\frac{1}{W}\frac{\partial}{\partial p}W. \quad (13)$$

The probability density $W(q,p,t)$ in the Gaussian kernel function can be rewritten as[45,46]

$$W(q,p,t)=\frac{1}{N}\sum_{j}^{N}\kappa_q(q-q_j(t))\kappa_p(p-p_j(t)), \quad (14)$$

where

$$\kappa_i(x)=\frac{1}{\sqrt{2\pi}h\sigma_i}\exp\Big\{-\frac{x^2}{2h^2\sigma_i^2}\Big\}, \quad (15)$$

with σ_i $(i=q,\ p)$ are the variance of q and p directions.

Finally, one could obtain the trajectories satisfying the equations[38–42]

$$\begin{aligned}&\dot{q}_j=\frac{p_j}{m},\\&\dot{p}_j=-V'-\gamma_0 p_j-\gamma_0 mk_{\mathrm{B}}T\frac{1}{W(q_j,p_j,t)}\frac{\partial}{\partial p}W(q_j,p_j,t).\end{aligned} \quad (16)$$

For the overdamped condition $\gamma_0\to\infty$, the corresponding Fokker–Planck equation reads[50]

$$\frac{\partial}{\partial t}W(q,t)=-\frac{\partial}{\partial q}\Big(-\mu V'(q)-D\frac{\partial}{\partial q}\Big)W(q,t), \quad (17)$$

and one could obtain the evolution equation of trajectories as follows:[31,50]

$$\dot{q}_j=-\mu V'-\frac{D}{W(q_j,t)}\frac{\partial}{\partial q}W(q_j,t), \quad (18)$$

where $D=\mu k_{\mathrm{B}}T$ is the diffusion coefficient, and the mobility $\mu=1/(m\gamma_0)$.

3. Results and discussion

In this section, we demonstrate the deterministic trajectory entropies of a particle traveling in harmonic potential and double-well potential in one- and two-dimensional conditions.

3.1. One-dimensional condition

We consider a particle traveling in viscous heat bath, with large friction constant γ_0. The motion of the particle can be described by the overdamped Langevin equation. The corresponding interacting trajectory method is employed to calculate the deterministic trajectory entropies.

3.1.1. Harmonic potential

The harmonic potential has been employed to describe many phenomena in solid state physics, atomic and molecular physics. Here, we consider the particle traveling in a harmonic potential, the harmonic potential is choose as $V(x)=\frac{1}{2}x^2$, and the initial condition is choose as

$$W(x)=\frac{1}{\sqrt{\pi}}\exp(-x^2). \quad (19)$$

The solution of the Fokker–Planck equation (17) under the initial condition is[51]

$$W(x,t)=\frac{1}{\sqrt{2\pi\sigma_s^2(t)}}\exp\Big[-\frac{x^2(t)}{2\sigma_s^2(t)}\Big], \quad (20)$$

with the time dependent variance

$$\sigma_s^2(t)=\frac{D}{2\mu}\Big[1-\Big(1-\frac{\mu}{D}\Big)\mathrm{e}^{-2\mu t}\Big]. \quad (21)$$

Substituting the analytical expression (20) into Eq. (1), one could obtain the Gibbs entropy

$$S(t)=\frac{1}{2}+\frac{1}{2}\ln\big[2\pi\sigma_s^2(t)\big]. \quad (22)$$

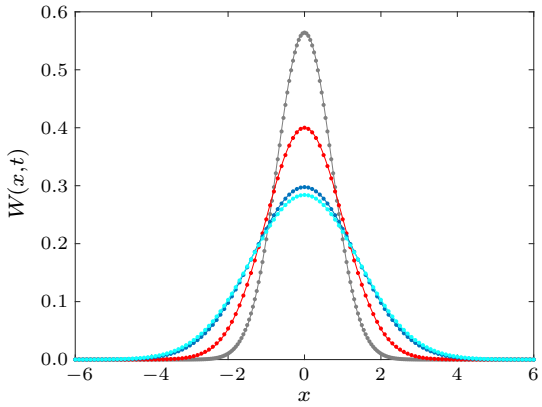


Fig. 1. Probability distributions of the particle moving in parabola potential, demonstrated at different times. The lines correspond to the result obtained by the interacting trajectory method and the dots are obtained by the analytical solution. Different colors correspond to different evolution times $t=0$ (grey), $t=0.2$ (red), $t=1$ (blue), and $t=2$ (cyan).

In our numerical calculation, we choose the diffusion coefficient $D=2$ and the mobility $\mu=1$, and the number of trajectories $N=200$. The probability distributions $W(x,t)$ at different times are demonstrated in Fig. 1. The solid lines correspond to the results obtained by the interacting trajectory method, and the dots stand for the results obtained by the analytical expression (20). The different colors correspond to different evolution times: $t=0$ (grey), $t=0.2$ (red), $t=1$ (blue), and $t=2$ (cyan). The probability distributions of the interacting trajectory method and the analytical expression are in agreement well with each other, which means that choosing $N=200$ in the interacting trajectory method is precise enough to obtain the distribution, and the corresponding entropies should be precise and reliable.

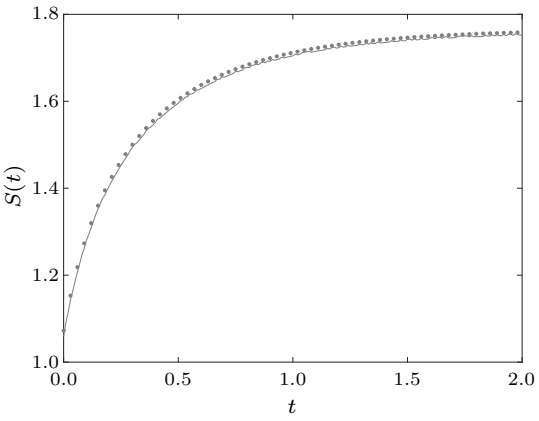


Fig. 2. Entropy averaged over all the trajectories versus the evolution time t. The solid line is obtained by the probability distribution with the Gaussian kernel estimation, and the dots are obtained by the analytical solution.

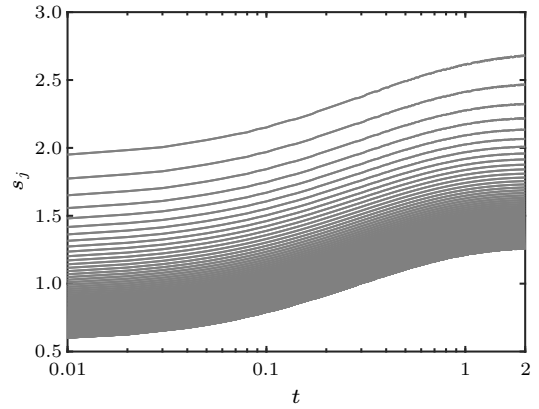


Fig. 3. Entropies of the trajectories versus the evolution time t. Different lines correspond different initial locations.

The Gibbs entropy $S(t)$ versus evolution time t are plotted in Fig. 2. The solid line corresponds to the result of the interacting trajectory approach, and the dots correspond to the analytical result. The result of the interacting trajectory approach is in agreement well with the analytical result (22). With the evolution time, the system finally reaches its steady state, and the corresponding Gibbs entropy $S(t)$ reaches a constant value.

The deterministic trajectory entropies $s_j(t)$ versus evolution time t are plotted in Fig. 3. The different solid lines correspond to the different initial conditions, and the deterministic trajectory entropies are "parallel" to each other, which can be thought such that there are no energy exchanging between trajectories. The increasing deterministic trajectory entropies $s_j(t)$ could be caused by absorbing heat from the thermal environment.

3.1.2. Double-well potential

The double-well model is generally used to describe the chemical reaction from the reactor to product, or the transition process from a state to the other state. We study deterministic trajectory entropies of a particle in double-well potential, and the double-well potential can be written as[39]

$$V(x) = \frac{a}{2}x^2 - \frac{b}{3}x^3 + \frac{c}{4}x^4, \tag{23}$$

where $a = 0.2$, $b = 0.3$, and $c = 0.1$. The minima positions of the potential appear at $x = 0$ and $x = 2$. The mass of the particle is chosen as $m = 2000$.[39]

We choose the system initially at its ground state

$$W(x) = \frac{1}{\sqrt{2\pi\sigma^2}} \exp\left(-\frac{x^2}{2\sigma^2}\right), \tag{24}$$

and the variance $\sigma = 1/\sqrt{40}$.

In the calculation, the friction constant is chosen as $\gamma_0 = 1/(2\pi)$, and the corresponding mobility $\mu \equiv 1/(m\gamma_0) = \pi \times 10^{-3}$, and $k_B T = 2.5 \times 10^{-2}$, and $D = \mu k_B T = 2.5 \times 10^{-5}\pi$.[39]

The probability distributions at different times are demonstrated in Fig. 4. The red dashed lines correspond to the results of the interacting trajectory method with $N = 200$, and the blue filled areas correspond to the results obtained by the Monte Carlo simulation method, the algorithms of the Monte Carlo simulation are accepted as in Ref. [52]. Firstly, the system initially in one of the potential well (say the left one), as the time increasing, some trajectories conquer the potential constraint and have reached the other potential well. With the time evolution, more and more trajectories have reached the other potential well, finally the system could reach its steady state and the distribution finally becomes the well-known Maxwell–Boltzmann distribution.

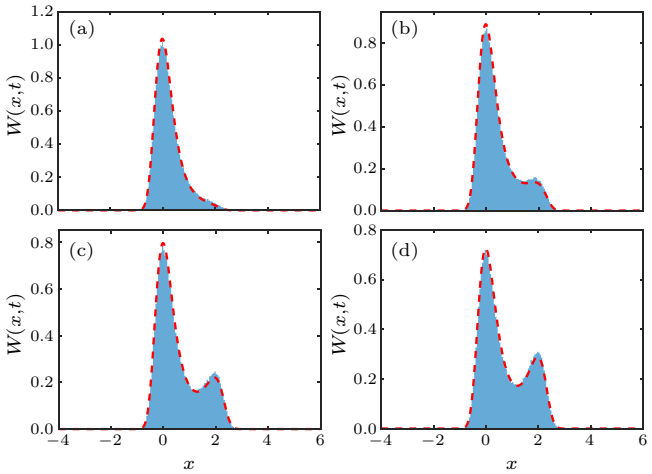


Fig. 4. Probability distributions at different times. The dashed red lines correspond to our interacting trajectory method, the blue bars are obtained by the Monte Carlo simulation method. The evolution times are (a) $t = 5000$, (b) $t = 10000$, (c) $t = 15000$, and (d) $t = 20000$.

The Gibbs entropy $S(t)$ versus evolution time t is plotted in Fig. 5. The blue dashed line corresponds to the result obtained by the interacting trajectory method, and the red solid line correspond to the result obtained by Monte Carlo simulation. In the short-time region, the Monte Carlo simulation method can not get enough evens and no enough data to obtain the Gibbs entropy $S(t)$. In the long-time region, the results obtained by interacting trajectory approach and Monte Carlo simulation method are consistent very well.

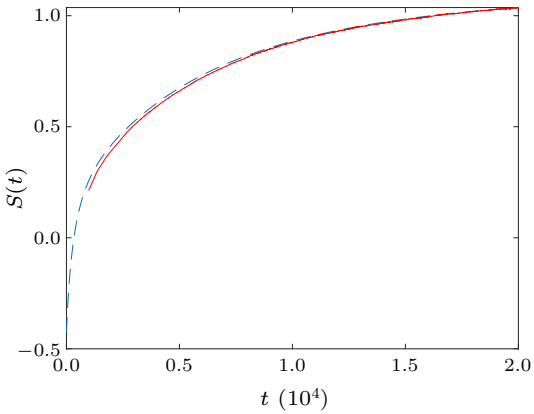


Fig. 5. Averaged entropy s versus evolution time t. The grey line corresponds to the result obtained by the interacting trajectory method, and the red dots correspond to the Monte Carlo simulation result.

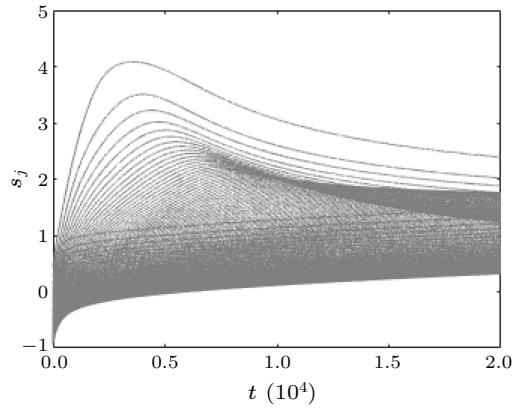


Fig. 6. Entropies of all the trajectories versus the evolution time t. The different initial conditions show different behaviors.

The deterministic trajectory entropies versus the evolution time t are plotted in Fig. 6. The deterministic trajectory entropy changes with evolution time t, and it reads[31]

$$\dot{s}_j(t) = -\frac{\partial_t W(x_j,t)}{W(x_j,t)} + \frac{j(x_j,t)}{DW(x_j,t)}\dot{x}_j(t) - \frac{\mu}{D}F(x_j,t)\dot{x}_j(t), \tag{25}$$

where $\partial_t \equiv \partial/\partial t$ represents the partial differential with respect to the evolution time t. Considering the probability flux

$$j(x_j,t) = \dot{x}_j(t)W(x_j,t), \tag{26}$$

one could have

$$\dot{s}_j(t) = -\frac{\partial_t W(x_j,t)}{W(x_j,t)} + \frac{1}{k_B T}[\gamma_0 m\dot{x}_j^2(t) - F(x_j,t)\dot{x}_j(t)], \tag{27}$$

where the first term on the right-hand side corresponds to the interaction among different trajectories as the $W(x_j,t)$ estimated by all trajectories; the term including $\dot{x}_j^2$ corresponds to the power of friction force, which always increases the entropy, and the last term corresponds to the power of conservative force $F(x_j,t)$ from the potential $V(x_j,t)$, which corresponds to the exchanging of the energy (heat) with the environment.[31]

The deterministic trajectory entropies are plotted in Fig. 6, the different lines correspond to different initial conditions. We have found that the deterministic trajectory entropies demonstrate two type behaviors: one is monotone increasing with evolution time t, which corresponds to the particle be confined in the initial well; the other is first increasing and then decreasing with evolution time t, which corresponds to the particle transition from one well to the other well. In the short-time region, the increasing entropies are caused by the system absorbing heat from the thermal environment, as the system initially in its ground state. The other trajectories, which have more kinetic energy, conquer the potential restriction to reach the maximum position of the potential, which causes the deterministic trajectory entropies still increasing with the evolution time t. After the trajectories over potential hill, the force works on the trajectories and the heat transfers back to the thermal environment, causing the deterministic trajectory entropies decreasing.

3.2. Two-dimensional condition

In this subsection, we consider the viscous constant being not large enough, the motion of the particle in potential can not be described by the overdamped Fokker–Planck equation.

3.2.1. Harmonic potential

We consider the particle with mass $m = 1$, traveling in the parabolic potential $V(q) = \frac{1}{2}q^2$, and choose the system initially in its ground state, namely,

$$W(q,p) = \frac{1}{\pi}\mathrm{e}^{-q^2}\mathrm{e}^{-p^2}, \tag{28}$$

the corresponding variances $\sigma_q^2 = 1/2$ and $\sigma_p^2 = 1/2$, which satisfy the minimum uncertainty condition $\sigma_q\sigma_p = 1/2$.

Two typical trajectories with different initial condition are plotted in Fig. 7. The stars represent the initial condition. The trajectories demonstrate the similar behaviors, i.e., spiral motion. As we all know, in phase space, the distance from the origin represents the energy of the particle. In Fig. 7, the trajectories rotation radius increases fast at the beginning time, which corresponds the energy of the trajectories increasing fast at the beginning time. This means that the trajectories absorb heat from the thermal environment, which causes the entropy of the trajectories also increasing fast at the beginning time. After the trajectories absorb enough heat from the the environment, the trajectories will reach the steady state. The entropy of the trajectories will also reach a constant value.

The Gibbs entropy $S(t)$ versus evolution time t is plotted in Fig. 8, the dashed line corresponds to result obtained by the interacting trajectory approach, and the solid line corresponds to the result of the difference equation of the Fokker–Planck equation. The Gibbs entropies, obtained by the interacting trajectory method and difference equation, demonstrate the similar behavior, namely, the Gibbs entropies increase fast with the

evolution time t at short time, then slowly increase with evolution time t and reach the steady state for the long-time limit. The difference between the results of the two methods at short time is caused by two parts, one is that the kernel estimation approach can not obtain precious probability distribution for the trajectories all close to each other, the other is that the difference equation (for fixed difference step) for the trajectories close condition can not give precious solution. With the time increasing, the trajectories become farther to each other, which makes the kernel estimation approach become more precious to obtain the probability distribution, also makes the Gibbs entropies obtained by the two different methods converged in long-time limit.

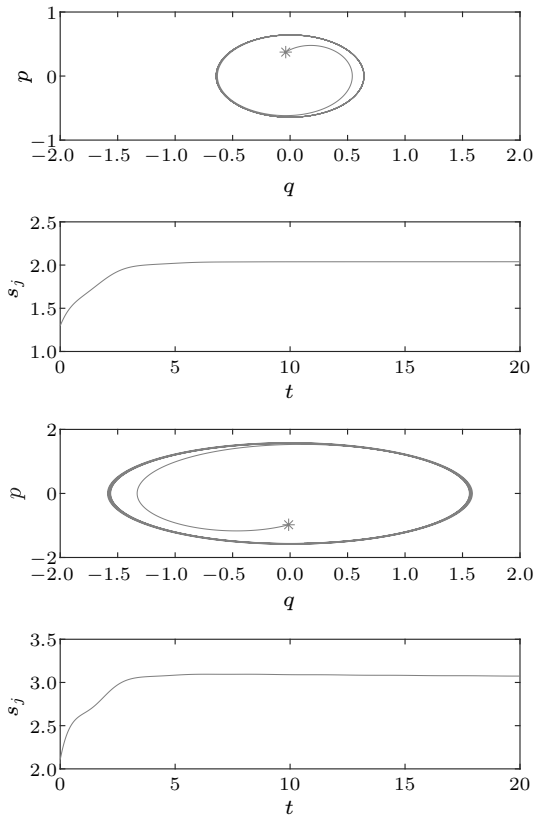


Fig. 7. Two typical trajectories and the corresponding entropies in phase space of the particle in the harmonic potential. The stars represent the initial points.

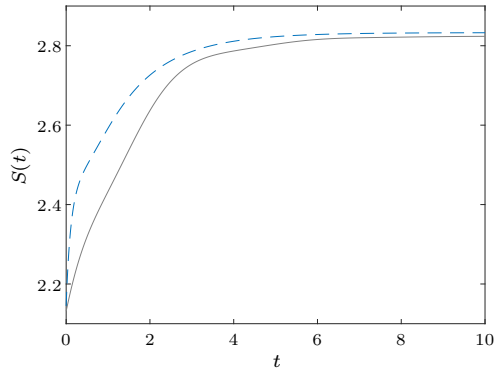


Fig. 8. Gibbs entropy $S(t)$ versus evolution time t. The solid line corresponds to the result obtained by the interacting trajectory approach, and the dashed line corresponds to the result obtained by the difference equation of the Fokker–Planck equation.

3.2.2. Double-well potential

We consider the double-well potential

$$V(q) = \frac{a}{2}q^2 - \frac{b}{3}q^3 + \frac{c}{4}q^4, \tag{29}$$

with $a = 0.2$, $b = 0.3$, $c = 0.1$. The minimum locations are at $q = 0$ and $q = 2$. In our numerical calculation, we choose the mass of the particle to be $m = 1$. The system is initially at $q = 0$ with the distribution

$$W(q,p) = \frac{1}{\pi}\mathrm{e}^{-q^2}\,\mathrm{e}^{-p^2}. \tag{30}$$

The corresponding variance $\sigma_q^2 = 1/2$ and $\sigma_p^2 = 1/2$, which satisfy the minimum uncertainty condition $\sigma_q\sigma_p = 1/2$.

Some typical trajectories in phase space of the particle moving in double-well potential are plotted in Fig. 9. The stars correspond the different initial conditions. From Fig. 9, one could find that there is three type trajectories: the first type is losing energy in the evolution process [see Figs. 9(a) and 9(d)]; the second type is the initial and the ending energy almost equal, but the energy "fluctuating" in the evolution process [see Fig. 9(b)]; and the last type is gain energy in the evolution process [see Figs. 9(c), 9(e), and 9(f)]. The trajectories exchange energies fast with other trajectories and thermal environment at the first several time units, the corresponding entropies are increasing fast at the same time region. In Fig. 9, we also demonstrate some interesting trajectories. In Figs. 9(d) and 9(f)], we find that the two trajectories seem not smooth enough at some points. The points reflect the collision between the trajectory with other trajectories, the trajectory is stopped by collision and then continuous moving in the same direction by the force exerting by the potential. Figure 9(c) shows the trajectory absorbing energy and losing energy fast at the first time, not having enough energy to conquer the potential "hill" and to reach the other potential well. Then the trajectory gains enough energy and reaches its steady state, transiting between the two potential wells.

The Gibbs entropy $S(t)$ is plotted in Fig. 10, the dashed line presents the result of the numerical solution of the Fokker–Planck equation, the solid line presents the result of the interacting trajectory method. The two results show same behavior, namely, monotone increasing with evolution time t. For the short-time region, the kernel estimation approach makes the probability distribution "diffusion" faster than that of the Fokker–Planck equation. For the long-time region, some trajectories are out of the sample region in numerical calculation, so that we can not completely calculate all the trajectories. This makes the difference of the entropies, obtained by the two different methods, at short time and long time.

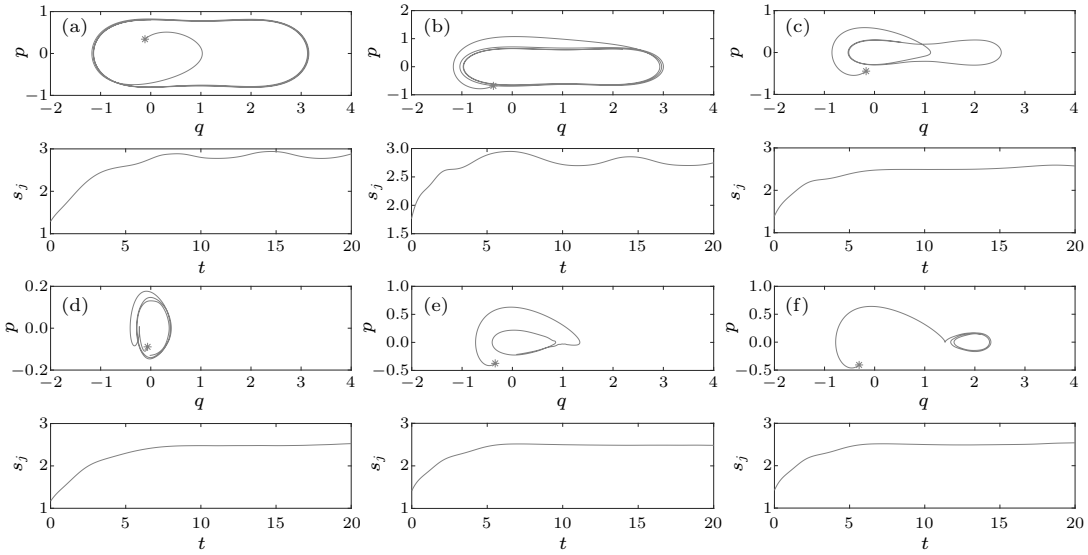


Fig. 9. Some trajectories and the corresponding entropies in phase space of the particle in double-well potential. The stars represent the initial points. [(a), (d), (b)] and [(c), (e), (f)] stand for the initial energy of the trajectory is less, equal, and greater than the finial energy, respectively. [(d), (e), (f)] The interesting trajectories interacting with other trajectories (the behavior can not be interpreted by classical trajectory theory).

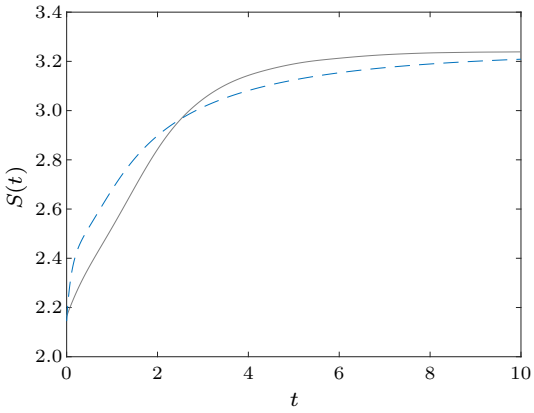


Fig. 10. Gibbs entropy $S(t)$ versus time. The solid line corresponds to the result obtained by the interacting trajectory approach, and the dashed line corresponds to the result obtained by the difference equation of the Fokker–Planck equation.

4. Conclusion

In this paper, we demonstrate the deterministic trajectory entropy of the particle traveling in two typical potentials (harmonic potential and double-well potential) with viscous environment by the interacting trajectory method. The harmonic potential and the double-well potential are investigated in one-dimensional space and two-dimensional space (phase space). The results obtained by the interacting trajectory approach are in agreement well with the Monte Carlo and difference equation methods. The deterministic trajectory entropies are increasing (decreasing) with the evolution time t, which corresponds to the trajectories absorption (emission) heat from (to) the thermal environment. Also, we demonstrate several interesting and rare trajectories in the process, which could help us to understand what is happened in the dynamical process in single-molecule level. Sometimes, the rare occurring even is important to stochastic processes, such as anomalous process. The study could help us to understand the anomalous process.

Acknowledgments

This work was supported by the National Natural Science Foundation of China (Grant No. 12234013) and the Natural Science Foundation of Shandong Province (Grant No. ZR2021LLZ009).

References

[1] Lemons D S 2013 *A Student's Guide to Entropy* (Cambridge: Cambridge University Press)
[2] Attard P 2002 *Thermodynamics and Statistical Mechanics: Equilibrium by Entropy Maximisation* (Cornwa: Academic Press)
[3] Sachs I, Sen S and Sexton J 2006 *Elements of Statistical Mechanics* (Cambridge: Cambridge University Press)
[4] Wehrl A 1978 *Rev. Mod. Phys.* **50** 221
[5] Huang K 1987 *Statistical Mechanics* 2nd Edn. (New York: Wiley)
[6] Chandler D 1987 *Introduction to Modern Statistical Mechanics* (Oxford: Oxford University Press)
[7] Gibbs J W 1960 *Elementary Principles in Statistical Mechanics* (New York: Dover Publications)
[8] Jaynes E T 1965 *Am. J. Phys.* **33** 391
[9] Zupanovic P and Kuic D 2018 *J. Phys. Commun.* **2** 045002
[10] Shannon C E 1948 *Bell System Tech. J.* **27** 379
[11] von Neumann J 1955 *The Mathematical Foundations of Quantum Mechanics* (Princeton: Princeton University Press)
[12] Haas K R, Yang H and Chu J W 2014 *J. Phys. Chem. B* **118** 8099
[13] Haas K R, Yang H and Chu J W 2014 *J. Phys. Chem. Lett.* **5** 999
[14] Weiderpass G A and Caldeira A O 2020 *Phys. Rev. E* **102** 032102
[15] Rossi M, Mancino L, Landi G T and Paternostro M 2020 *Phys. Rev. Lett.* **125** 080601
[16] Klages R, Just W and Jarzynski C (eds) 2013 *Nonequilibrium Statistical Physics of Small Systems* (Weinheim: Wiley-VCH Verlag)
[17] Holian B L 1986 *Phys. Rev. A* **33** 1152
[18] Grandy and Jr W T 2008 *Entropy and the Time Evolution of Macroscopic Systems* (New York: Oxford University Press)
[19] Kleidon A and Lorenz R D (eds) 2005 *Non-Equilibrium Thermodynamics and the Production of Entropy: Life, Earth, and Beyond* (Berlin: Springer-Verlag)
[20] Seifert U 2012 *Rep. Prog. Phys.* **75** 126001
[21] Sekimoto K 1998 *Prog. Theor. Phys. Suppl.* **130** 17

[22] Evans D J, Cohen E G D and Morriss G P 1993 *Phys. Rev. Lett.* **71** 2401
[23] Evans D J and Searles D J 1994 *Phys. Rev. E* **50** 1645
[24] Gallavotti G and Cohen E G D 1995 *Phys. Rev. Lett.* **74** 2694
[25] Seifert U 2005 *Europhys. Lett.* **70** 36
[26] Kurchan J 1998 *J. Phys. A: Math. Gen.* **31** 3719
[27] Jarzynski C 1997 *Phys. Rev. Lett.* **78** 2690
[28] Crooks G E 1999 *Phys. Rev. E* **60** 2721
[29] Hatano T and Sasa S i 2001 *Phys. Rev. Lett.* **86** 3463
[30] Qian M 1985 *Chin. Sci. Bull.* **30** 165 (in Chinese)
[31] Seifert U 2005 *Phys. Rev. Lett.* **95** 040602
[32] Tietz C, Schuler S, Speck T, Seifert U and Wrachtrup J 2006 *Phys. Rev. Lett.* **97** 050602
[33] Mandal D, Klymko K and DeWeese M R 2017 *Phys. Rev. Lett.* **119** 258001
[34] Bunker D L 1971 *Methods Comput. Physics: Adv. Res. Appl.* **10** 287
[35] Sanz A S and Miret-Artes S 2012 *A Trajectory Description of Quantum Processes* (Berlin: Springer)
[36] Chattaraj P K (ed) 2010 *Quantum Trajectories* (Boca Raton: CRC Press)
[37] Wyatt R E and Trahan C J 2005 *Quantum Dynamics with Trajectories* (Berlin: Springer)
[38] Donoso A and Martens C C 2001 *Phys. Rev. Lett.* **87** 223202
[39] Donoso A and Martens C C 2002 *J. Chem. Phys.* **116** 10598
[40] Sun Z, Dong H and Zheng Y 2018 *Phys. Rev. E* **97** 012132
[41] Xu F, Martens C C and Zheng Y 2017 *Phys. Rev. A* **96** 022138
[42] Wang L, Martens C C and Zheng Y 2012 *J. Chem. Phys.* **137** 034113
[43] Attard P 2012 *Non-Equilibrium Thermodynamics and Statistical Mechanics* (Oxford: Oxford University Press)
[44] Brewster R A and Frason J D 2018 *J. Math. Phys.* **59** 012102
[45] Wand M P and Jones M C 1995 *Kernel Smoothing* (New York: Springer)
[46] Silverman B W 1998 *Density Estimation for Statistics and Data Analysis* (New York: Chapman & Hall)
[47] Kramers H A 1940 *Physica* **7** 284
[48] Kubo R, TodaMand hashitsume N 1985 *Statistical Physics Ⅱ: Nonequilibrium Statistical Mechanics* (Berlin: Springer-Verlag)
[49] Gardiner C W 2004 *Handbook of Stochastic Methods* 3rd Edn. (Berlin: Springer-Verlag)
[50] van Kampen N G 2007 *Stochastic Processes in Physics and Chemistry* 3rd edn (Singapore: Elsevier)
[51] Risken H 1996 *The Fokker–Planck Equation* 2nd Edn. (Berlin: Springer-Verlag)
[52] Jacobs K 2010 *Stochastic Processes for Physicists - Understanding Noisy Systems* (Cambridge: Cambridge University Press)